Preprint Title	Photoswitchable glycoligands targeting *Pseudomonas aeruginosa* LecA
Authors	Yu Fan, Ahmed El Rhaz, Stéphane Maisonneuve, Emilie Gillon, Maha Fatthalla, Franck Le Bideau, Guillaume Laurent, Samir Messaoudi, Anne Imberty and Juan Xie
Publication Date	20 März 2024
Article Type	Full Research Paper
Supporting Information File 1	SI.pdf; 6.5 MB
ORCID® iDs	Ahmed El Rhaz - https://orcid.org/0009-0003-1772-1699; Stéphane Maisonneuve - https://orcid.org/0000-0003-0459-3459; Franck Le Bideau - https://orcid.org/0000-0003-4365-4525; Samir Messaoudi - https://orcid.org/0000-0002-4994-9001; Anne Imberty - https://orcid.org/0000-0001-6825-9527; Juan Xie - https://orcid.org/0000-0001-7664-5532

Photoswitchable glycoligands targeting *Pseudomonas aeruginosa* LecA

Yu Fan[1], Ahmed El Rhaz[2], Stéphane Maisonneuve[1], Emilie Gillon[3], Maha Fatthalla[2], Franck Le Bideau[2], Guillaume Laurent[1], Samir Messaoudi[4], Anne Imberty[3*], and Juan Xie[1]*

[1]Université Paris-Saclay, ENS Paris-Saclay, CNRS, Photophysique et Photochimie Supramoléculaires et Macromoléculaires, 91190, Gif-sur-Yvette, France.

[2]Université Paris-Saclay, CNRS, BioCIS, 92290, Orsay, France
[3]CERMAV, University Grenoble Alpes, CNRS, 38000 Grenoble, France
[4]Laboratoire de Synthèse Organique, Ecole Polytechnique, CNRS, ENSTA, Institut Polytechnique de Paris 91128 Palaiseau, France

Corresponding autors email: joanne.xie@ens-paris-saclay.fr; anne.imberty@cermav.cnrs.fr

Keywords: Carbohydrates; Glycosyl azobenzenes; Lectin A; photoswitchable ligands

Abstract

Biofilm formation is one of main causes of bacterial antimicrobial resistance infections. It is known that the soluble lectins LecA and LecB, produced by *Pseudomonas aeruginosa*, play a key role in biofilm formation and lung infection. Bacterial lectins are therefore attractive targets for the development of new antibiotic-sparing anti-infective drugs. Building synthetic glycoconjugates for the inhibition and modulation of bacterial lectins have shown promising results. Light-sensitive lectins ligands could allow the modulation of lectins activity with precise spatiotemporal control. Despite the potential of photoswitchable tools, few photochromic lectin ligands have been developed. We have designed and synthesized several *O*- and *S*-galactosyl azobenzenes as photoswitchable ligands of LecA and evaluated their binding affinity with isothermal titration calorimetry. We show that the synthesized monovalent glycoligands possess excellent photophysical properties and strong affinity for targeted LecA with K_d values in the micromolar range. Analysis of the thermodynamic contribution indicates that the *Z*-azobenzene isomers have systematically stronger favorable enthalpy contribution than the corresponding *E*-isomers, but due to stronger unfavorable entropy, they are in general of lower affinity. The validation of this proof-of-concept and the dissection of thermodynamics of binding will help for the further development of lectins ligands that can be controlled by light.

Introduction

Bacterial infection is a growing health problem due to antimicrobial resistance (AMR) among others. AMR causes approximately 33,000 deaths per annum in Europe only, [1] and costs between €1.5 and €9 billion in healthcare and associated activities. Many bacterial infections occur by adhesion to host tissues through receptor-ligand interaction between bacterial carbohydrate-binding proteins (lectins) and oligosaccharides at the host cell surface. *Pseudomonas aeruginosa* (PA), *a* Gram-negative, opportunistic and ubiquitous environmental bacterium, is known as the leading cause of morbidity and mortality in cystic fibrosis and immunocompromised patients and as one of the leading causes of nosocomial infections. [1] Due to the existence of numerous molecular mechanisms conferring resistance to multiple classes of antibiotics, therapeutic options are increasingly limited for treatment of infections. PA has been classified as a Priority 1 pathogen by the WHO. [2,3] Various approaches to treating PA, in addition to traditional antibiotics, have been developed including inhibition of quorum sensing, biofilm-formation, iron chelation and interfering with biosynthetic pathways of the bacterium. [2,3] Soluble

lectins LecA and LecB produced by PA play a key role in the infection. [4] PA LecA is demonstrated to be crucial for biofilm formation and internalization, while the extracellular LecB plays a key role in bacterial adhesion to the host and biofilm formation. [5-8] Building synthetic glycoconjugates for the inhibition and modulation of bacterial lectins responsive for biofilm formation have shown promising results. [9,10] Unlike antibiotics, lectin inhibitors could prevent pathogenicity by interfering with virulence factors instead of killing the bacteria. Bacterial lectins are therefore attractive targets for the development of new antibiotic-sparing anti-infective drugs. For example, some *Escherichia coli* fimbrial lectin FimH inhibitors are currently in clinical development to treat and prevent urinary tract infections. [9,10] Large number of glycomimetic inhibitors of PA LecA and LecB have also been reported, with anti-biofilm formation activity for some of them. [5-8]

Photochromic molecules, which may be reversibly converted between different isomers upon illumination, offer numerous opportunities for reversibly photomodulating chemical, biological or pharmacological activities or properties. [11,12] Light is generally noninvasive and orthogonal toward most elements of living systems. It can be easily and precisely controlled in time, location, wavelength and intensity, thus enabling the precise activation and deactivation of biological function. It also offers the potential to change the properties of defined molecules in biological systems with minimal disturbance to the rest of the system. There is an increasing use of the photoisomerization to control the conformation as well as the activities of various biomolecules with the development of photopharmacology. [11-16] The group of Lindhorst has reported a series of mannosyl azobenzenes targeting *E. Coli* lectin FimH, demonstrating the possibility to control the type 1 fimbriae-mediated bacterial adhesion to a self-assembled monolayers of mannosyl azobenzene on a gold surface [17,18] or to mannosylazobenzene-modified human cells [19] through photoswitching the orientation of the attached mannoside [20]. Photoswitchable glycooligomers [21] or glycodentrimers [22] have been investigated for the inhibition of PA lectin PA-IL or LecA and LecB. A variation of IC_{50} value by a factor up to 1.6 has been observed for the divalent ligand [21]; while almost no difference of inhibition was observed for LecA and LecB upon irradiation, probably due to the low photoisomerization of glycodentrimers [22]. Very recently, the group of Wittmann reported an arylazopyrazole-linked divalent *N*-acetylglucosamine targeting lectin wheat germ agglutinin [23]. The binding affinity k_d evaluated by isothermal titration calorimetry (ITC) showed a variation by a factor of 12.5 upon the photoisomerization. However, direct photo modulation of monovalent lectin ligand has not been achieved up to date. Based on our experiences in photoswitchable glycosides and bacterial lectins, [4,6-8,24-29] we have designed, synthesized and characterized the first generation of *O*- and *S*-galactosyl azobenzenes as photoswitchable monovalent ligands targeting PA LecA. Their binding affinity with LecA evaluated by isothermal titration calorimetry (ITC) showed K_d values in micromolar range with significant thermodynamics difference between *E*- and *Z*-azobenzene isomers, demonstrating the proof-of-concept of photomodulation of the ligand-lectin interactions.

Results and Discussion

Design of LecA photoswitchable ligands

The cytotoxic LecA which has a tetrameric structure, displays a high affinity for D-galactose (D-Gal, with K_d = 34 μM) and galactosides. The 3- and 4-hydroxyl function on the D-Gal unit are involved in the coordination of Ca^{2+} in the binding site. [5-8,30] A large range of galactosyl conjugates have been synthetized, with k_d value from micromolar (for monovalent galactosides) to nanomolar ranges (for di- and multivalent derivatives). [5-8] For the monovalent system, it has been shown that aromatic aglycons

favored "T-shaped" CH···π interactions with the protons of the His50 imidazole in the carbohydrate-binding pocket, with the *β*-linked aromatic aglycons having five-fold higher affinity compared to aliphatic analogues. [31,32] Beside *β*-O-aryl galactosides, enzymatically more stable *β*-S-aryl galactosides have also been successfully developed as monovalent LecA ligands (Figure 1A). [28,33] Since different sizes and substituents are tolerated on the aryl aglycon, we decided to replace the aryl aglycon by photoswitchable azobenzene in both *O*- and *S*-galactosides (Figure 1B) to investigate their binding affinity and the influence of the photoisomerization on the lectin interaction. The ammonium group is introduced on the azobenzene to increase the water solubility. The influence of *ortho*, *meta* and *para*-substitution pattern of the azobenzene on the lectin binding has also been studied.

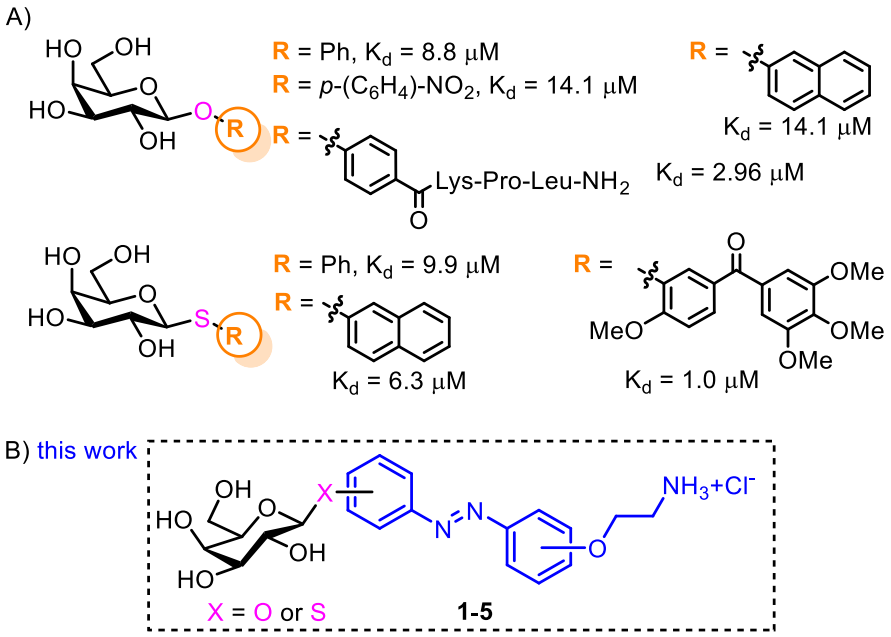

Figure 1. (A) Selected monovalent inhibitors for PA LecA; (B) Designed general structure of photoswitchable ligands targeting LecA **1-5**.

Synthesis

The *β*-O-galactosyl *p,p*-bis-substituted azobenzene derivative **1** was prepared from galactose and commercially available *p,p'*-bishydroxy azobenzene **6**, by using our recently developed DMC (2-chloro-1,3-dimethylimidazolinium chloride)-mediated one-pot glycosylation method in water, [26] followed by *O*-alkylation of the remaining hydroxyl group with $BrCH_2CH_2NHBoc$ and acidic deprotection (Scheme 1). 3 equivalents of bishydroxy azobenzene **6** were used for the selective mono-glycosylation step, with the excess of azobenene being recovered after column chromatography. The same strategy was applied for the *m,m'*-substituted derivative **2**, starting from the glycosylation of *m,m'*-bishydroxy azobenzene **9**, [34] followed by *O*-alkylation and Boc deprotection to afford the galacoside **2** in 19% total yield. Unfortunately all our attempts to synthesize the *o,o'*-bis-substituted derivative failed. For the *β*-S-galactosyl azobenzene derivatives which are accessible by our previously reported Pd-catalyzed cross-coupling methodology between glycosyl thiols and iodoaryl partners, [28,35] the required *p*-, *m*- or *o*-iodo-*p'*-hydroxy-azobenzenes (**12, 17** and **21**) were prepared by the diazonium coupling method according to a reported procedure. [36,37] Then the coupling with tetra-*O*-acetylated *β*-galactosylthiol **13** catalysed by Xantphos Pd-G_3 [35] precatalyst followed by post-functionalisation furnished the desired *β*-S-galactosyl azobenzenes **3-5** in 37-71% total yields (Scheme 1).

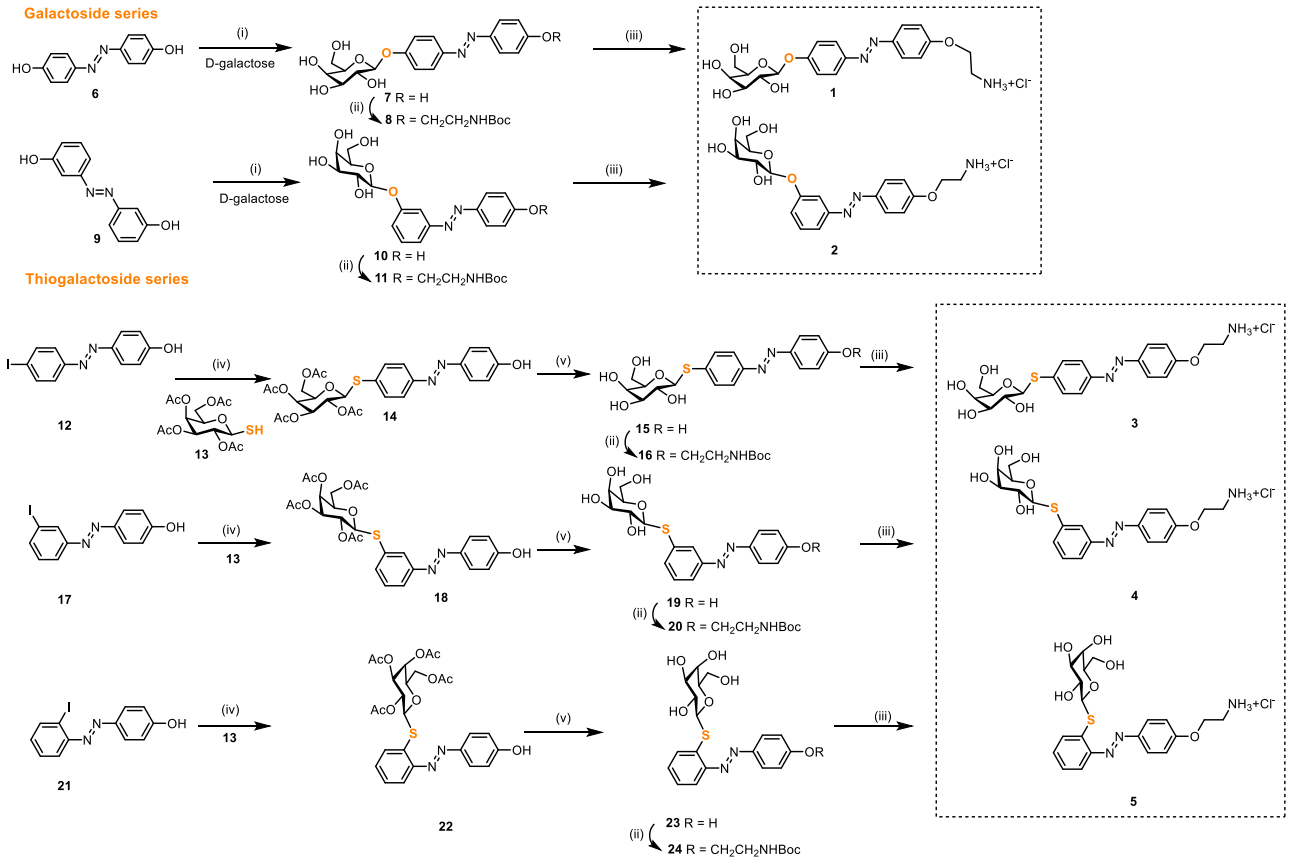

Scheme 1. Synthesis of photoswitchable LecA inhibitors. Reagents and conditions: (i) DMC, Et_3N, H_2O, -10 °C to rt, 8h, 50% for **7**, 40% for **10**; (ii) $BrCH_2CH_2NHBoc$, K_2CO_3, DMF, 60 °C, 15h, 91% for **8**, 80% for **11**, 88% for **16**, 50% for **20**, 88% for **24**; (iii) AcCl, MeOH, 0°C to rt, 15h, 58% for **1** and **2**, 90% for **3**, 85% for **4**, 77% for **5**; (iv) Xantphos Pd-G_3 (5 mol%), Et_3N, THF, 6-8 h, rt 90% for **14**, 98% for **18**, 54% for **22**; (v) MeONa/MeOH, 30 mn-2 h, rt >99% for **15**, **19** and **23**.

Photophysical characterization

The photoswitching properties of galactosyl azobenzenes **1-5** were realized in water or in Tris buffer containing 5 to 10% DMSO, in accordance with the biophysical evaluation conditions by using ITC. All these compounds underwent readily reversible photoisomerization under UV-visible irradiation in aqueous solution. As shown in Figure 2, the *O*-galactosyl azobenzene **1** underwent reversible photoisomerization under UV (370 nm) and visible (485 nm) irradiations in water, with a high fatigue resistance as no degradation has been observed after more than 10 irradiation cycles (Figure 2). It showed a relatively strong $\pi \rightarrow \pi^*$ transition (λ_{max} = 353 nm) and a weaker forbidden $n \rightarrow \pi^*$ transition ($\lambda_{max} \approx$ 440 nm) (Figure 2, black line). Irradiation at 370 nm resulted in the decrease of the band at 353 nm and appearance of new bands at 312 and 438 nm, revealing the *E* to *Z* isomerization (Figure 2, blue line). Two isosbestic points can also be observed at 310 and 429 nm. The back $Z \rightarrow E$ photoisomerization can be achieved by illumination at 485 nm (Figure 2, red line). Varying *Z*/*E* ratios during irradiation can be determined by ^1H NMR, with an excellent photoconversion yield of *Z*/*E* = 99/1 at PSS_{370}, and *E*/*Z* = 87/13 at PSS_{485} in D_2O (Figure 3). The *Z*-isomer is thermostable, with the half-life determined to be 44.4 h in water at room temperature (Figure S9). The photophysical properties of compounds **1-5** are summarized in Table 1 (Figures S1 to S24). For the *meta*-substituted azobenzene **2**, a blue-shifted of 30 nm for the $\pi \rightarrow \pi^*$ transition (λ_{max} = 321 nm) and a lower absorption coefficient have been observed compared to the *para*-derivative **1** (Table 1, entries 3,4 *vs* entries 1,2) probably due to less-conjugated azobenzene. The better $Z \rightarrow E$ photoconversion was achieved by illumination at 438 nm instead of 485 nm. An increased thermostability has also been observed ($t_{1/2}$ = 29 days) for **2**. The *S*-galactosyl azobenzenes **3-5** also displayed excellent photoswitching properties, with a red-shift for the $\pi \rightarrow \pi^*$ transition (λ_{max} = 348-364 nm) compared to the *O*-galactosyl derivatives (Table 1, entries 5-8). However,

the absorption coefficient and the thermostability of the *Z*-isomers are highest for the *meta*-derivative (**4**), compared to the *ortho*- (**5**) and *para*-substituted **3**.

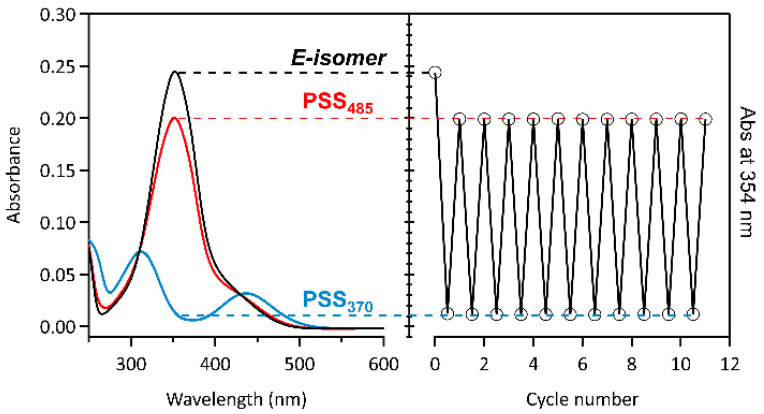

Figure 2 (Left) Absorption spectra and (right) fatigue resistance of **1** under alternated 370/485 nm irradiations in Tris buffer: DMSO (95:5) at rt: *E*-**1** (black line), PSS_{370} (blue line), PSS_{485} (red line). Irradiation condition at 370 nm: 12.8 mW·cm^{-2}, 20 s; at 485 nm: 1.5 mW·cm^{-2}, 480 s.

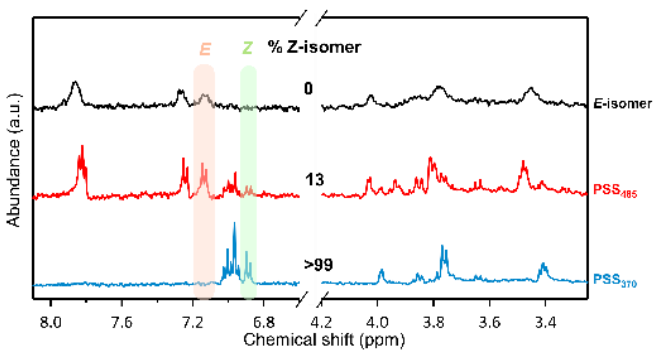

Figure 3. ^{1}H NMR spectra of *E*-**1** (black line), PSS_{370} (red line), PSS_{485} (blue line) in D_2O.

Table 1. Steady-state absorption, photostationary state composition and half-life of *Z*-isomers of **1**-**5**.

Entry	Compound	Solvent	Ɛ [M^{-1}cm^{-1}]	λ_{max} [nm]	*Z*/*E* PSS_{370}	*E*/*Z* PSS_{485}	$t_{1/2}$
1	**1**	H_2O	25632	353	99/1	87/13	44.4 h
2		Tris[a]-DMSO 5%	24400	354	n.d.[b]	n.d.	n.d.
3	**2**	Tris-DMSO 5%	14155	321	87/13	71/29	29.1 d[d]
4		Tris-DMSO 10%	15288	321	87/13	74/26[c]	n.d.
5	**3**	H_2O	18111	362	99/1	73/27	30.4 h
6		Tris-DMSO 10%	16991	364	99/1	71/29	25.9 h
7	**4**	Tris-DMSO 10%	22358	348	99/1	72/28	9.0 d
8	**5**	Tris-DMSO 10%	17336	348	92/8	60/40	73.3 h

[a]Tris buffer: Tris 20 mM (pH = 7.5), NaCl 100 mM, $CaCl_2$ 100 µM. [b]not determined. [c]PSS_{438} for **2**. [d]days.

Biophysical evaluation by ITC

The interaction of compounds **1**-**5** with LecA was characterized by ITC analysis for both the *E*- and *Z*-isomers. As the initial isomer state of the galactosyl azobenzenes is the *E*-form, ITC measurements made on *E*-isomers correspond to 100% purity of it. After 370 nm irradiation to induce the photoizomerisation process, a photostationary state is reached between *E*- and *Z*-isomers. For ITC measurements made on *Z*-isomers, the percentage of isomers is shown in the column *Z*/*E* (PSS_{370}) of the Table 1. Depending on the corresponding galactosyl azobenzenes, *Z*-isomer is pure from 87 to 99%. Spectroscopy measurements were performed on ligand solution just before each experiment to check the efficiency of the isomerization, with results as indicated in Table 2. In all experiments, strong exothermic peaks were observed for the first injection, followed by titration corresponding to stoichiometry of 1, in agreement with known structure (Figure 4). Control experiment with injection of compounds in buffer only did not show significant heat of dilution.

Affinity values, as well as thermodynamics contribution could be extracted through fitting procedure with a one site model and data are reported in Table 2. All compounds have strong affinity for LecA with k_d values ranging from 1.9 µM to 13.6 µM. These values are in the range of those observed previously for aromatic galactoside derivatives, [31,32] confirming the favorable interaction of the aryl group with the protein surface. For all compounds, no significant differences of affinities are observed between *E*- and *Z*-isomer, with the exception of compounds **1** and **3** with *para* orientation between the two aryl groups. The affinity of the *E*-isomer is twice better than for its *Z*-counterpart for the *S*-linked compound (**3**) and three times better for the *O*-glycoside (**1**). Even though the other compounds do not exhibit significant variations of affinities between *E*- and *Z*-isomers, a closer look at the thermodynamic values indicates that the mechanisms of binding display significant variations (Table 2). All of the *Z*-isomers display stronger favorable enthalpy of binding, *i.e.* a more negative ΔH contribution (ΔH varying from -41.1 to -49.4 kJ/mol) than their *E*-counterpart (ΔH from -38.0 to -43.5 kJ/mol). This is fully counterbalanced by a stronger unfavorable entropy barrier, *i.e.* a more positive entropy contribution (-TΔS). Varying from 10.3 to 18.5 kJ/mol for the *Z*-isomers, and from 8.8 to 13.1 kJ/mol for the *E*-isomers. As displayed in Figure 4, this enthalpy-entropy compensation results in limited variation of ΔG and therefore in the observed rather similar K_d values.

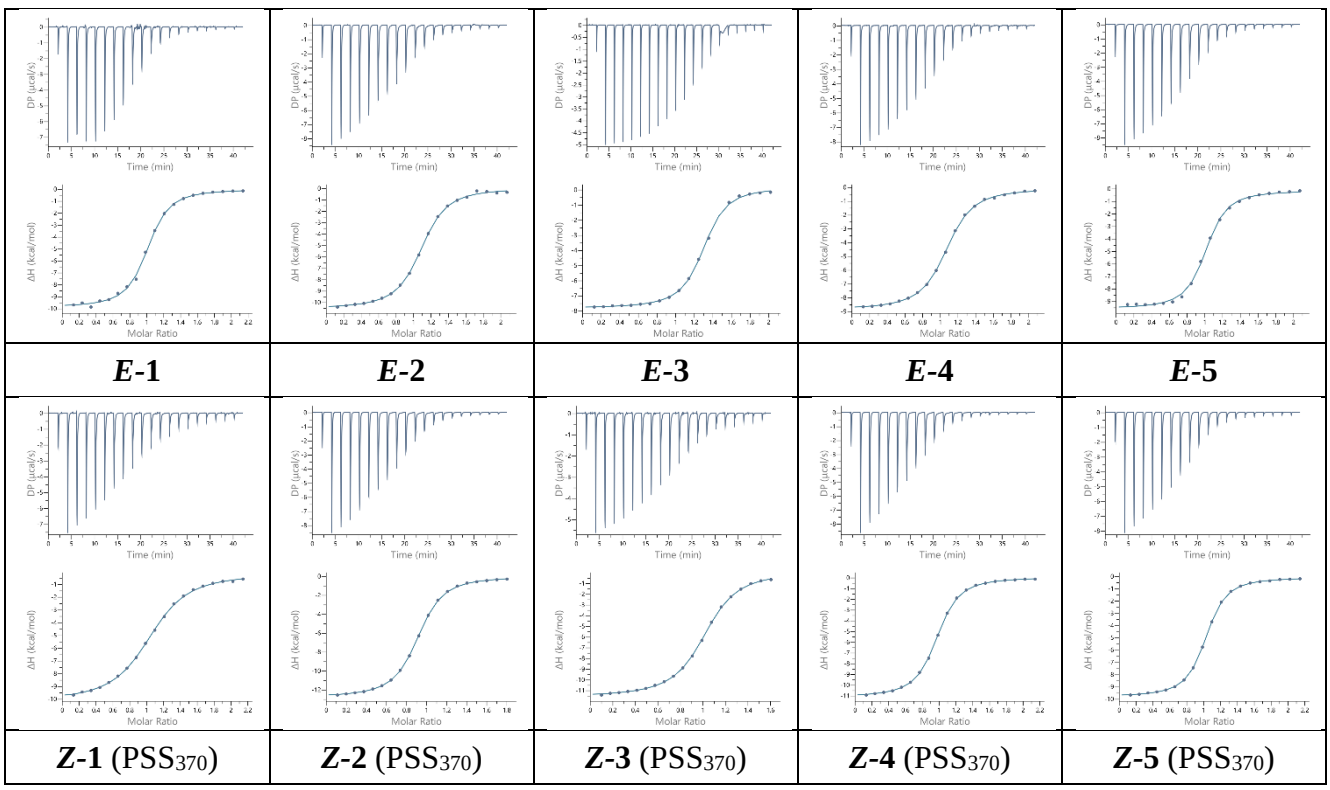

Figure. 4 ITC titration of LecA with *E*- (up) and *Z*-isomers (bottom) of compounds **1**-**5** in Tris buffer containing 5 to 10% DMSO. The plot in the lower panel shows the total heat released as a function of total ligand concentration for the titration shown in the upper panel. The solid line represents the best least-square fit to experimental data using a one site model.

Table 2. Microcalorimetry data and thermodynamics contribution for binding to LecA. The experiments were realized in duplicate at 298 K unless otherwise stated.

Ligand	K_d [μM]	n	-ΔG [kJ/mol]	-ΔH [kJ/mol]	TΔS [kJ/mol]
***E*-1**	4.8±0.3	0.98±0.01	30.3	40.8±0.5	-10.5
***Z*-1**	13.6±1.2	1.04±0.04	27.8	41.3±0.5	-13.5
***E*-2**	5.1±0.7	1.01±0.05	30.2	43.3±1.0	-13.1
***Z*-2**[a]	5.1±0.7	0.97±0.04	30.2	45.8±0.6	-15.6
***E*-3**	1.9±0.1	1[b]	32.6	43.5±0.4	-10.9
***Z*-3**	4.1±0.02	1[b]	30.7	49.4±0.4	-18.7
***E*-4**	7.7±1.3	0.96±0.07	29.2	38.0±1.3	-8.8
***Z*-4**	5.1±0.1	0.96±0.02	30.2	47.1±0.2	-16.9
***E*-5**	4.3±0.2	1.02±0.05	30.6	40.1±0.6	-9.5
***Z*-5**[a]	4.1±0	0.96±0.03	30.8	41.1±0.4	-10.3

[a]*Z*-isomer of compound **2** is mixed with 13% *E*-isomer and compound **5** is mixed with 8% *E*-isomer as established by PSS_{370}. This contamination is less than 2% for the other compounds. [b]Concentration of compound **3** could not be determined from weight products due to aggregation. Active concentration was determined fitting ITC data to stoichiometry of 1, value confirmed from other compounds. For all other compounds, concentration was calculated from weighted compound and confirmed by spectroscopy (see Table S1 in Supp info).

In order to rationalize this difference in binding mechanism, molecular models were obtained for selected low energy conformations of *E* and *Z* isomers of a "model" scaffold of the *para*-azobenzene derivative in the binding site of LecA, by simple superposition on known crystal structure. The extended *E*-isomer establishes contact through galactoside and the first aryl ring only, while bended *Z*-isomer has proper conformation to wrap around the central His53 residue and to establish more extended interaction with protein surface. This would be in agreement with stronger enthalpy of interaction, while the entropy barrier could arise from limitation of flexibility and/or blocking of water molecules at the new interface.

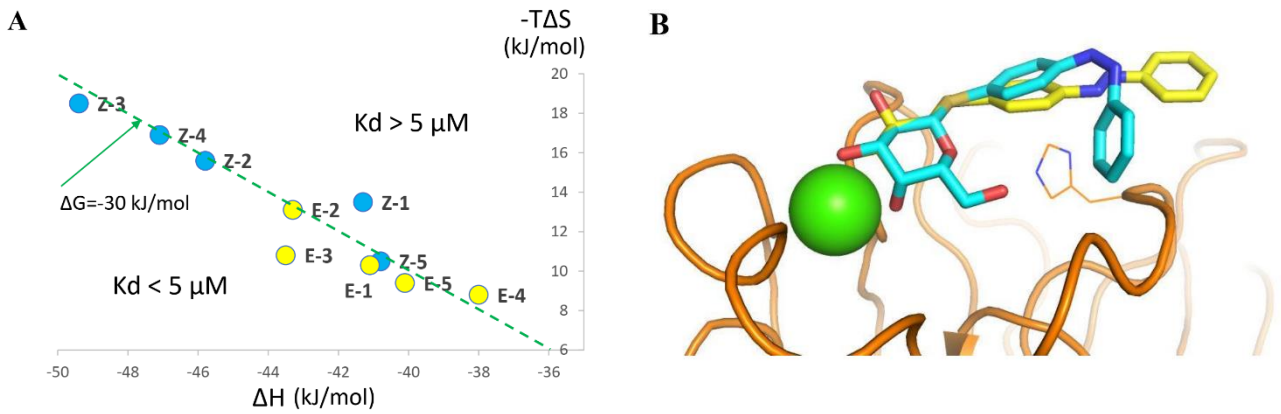

Figure 5. (A) Enthalpy-entropy compensation plot of compounds **1-5** from ITC analysis. The dotted green line represents a ΔG value of -30 kJ/mol, corresponding to a K_d of approx 5 μM in the experimental conditions. (B) Manual docking of scaffold for compound **3** with selected low energy conformations of *E*-isomer (yellow sticks) and *Z*-isomer (cyan sticks) superimposed on conserved position of galactose in all LecA crystalline complexes. The protein is represented by orange ribbon, His53 by lines and calcium by green sphere.

Conclusion

We have designed and synthesized in three to five steps *O*- and *S*-galactosyl azobenzenes targeting the Pseudomonas aeruginosa lectin LecA. The five synthesized glycoconjugates can be reversibly photoconverted between *E* and *Z* isomers under UV and Vis irradiation, with good to excellent

photoconversion yields, and high fatigue resistance in aqueous media. Furthermore, all the Z-isomers displayed good thermostability, with the half-live varied from 26 h to 29 days at room temperature depending on the type of glycosidic linkage and the substitution pattern on the azobenzene moiety. The bistability of the azobenzene derivatives is suitable for the investigation of azobenzene isomers on the binding affinity with LecA. All the galactosyl azobenzenes bound to LecA in the low micromolar range. Interestingly, the *para*-substituted *O*- (**1**) and *S*- (**3**) galactosides displayed 2 to 3-fold difference in affinity between *E* and *Z* isomers (3-fold difference for **1** and 2-fold for **3**), demonstrating the proof-of-concept of tuning the LecA binding by light. Few differences were observed for the *meta*- (**2** and **4**) and *ortho*-substituted azobenzenes (**5**). Thermodynamics contributions exhibit larger variations with stronger enthalpy of binding for the Z-isomer, probably in relation with folded conformation generating additional contact with the surface. Due to enthalpy-entropy compensation, that is a general effect in protein-carbohydrate interactions, [38] this does not reflect in differences in affinity. However, these observations, together with future modeling study, will help in designing future compounds with more selective binding of one isomer only.

Experimental

General Experimental Details. Commercially available solvents and reagents were used without further purification. The reactions carried out under anhydrous conditions are performed under argon in glassware previously dried in an oven. DMF and THF were previously dried through alumina or molecular sieves cartridge using a solvent purificator MBRAUN SPS-800. All the reactions with azobenzene-containing substrates were carried out in the dark. Reactions were monitored by TLC on Silica Gel 60F-254 plates with detection by UV (254 nm or 365 nm) or by spraying with 10% H_2SO_4 in EtOH and heating about 30 s at 400-600 °C. Column chromatography purification was performed on CombiFlash® Rf+ and RediSep® RF or RF Gold normal phase silica columns (with UV detection at 254 and 350 nm for all azobenzene-derivatives), or by flash column chromatography employing silica gel (60 Å pore size, 40-63 µm). ^{1}H and ^{13}C-NMR spectra were recorded on a JEOL ECS-400 spectrometer or on Bruker Avance 300 and 400 spectrometers. Structural assignments were made with additional information from gCOSY, HMBC and gHMQC experiments. High-resolution mass spectra (HRMS) were performed on a Bruker maXis mass spectrometer by the SALSA platform from ICOA laboratory or on an Agilent 1260 Infinity system with a quadrupole time-of-light (Q-TOF) mass analyser. Melting points were measured with a Köfler bench previously calibrated using the usual standard references or on a digital melting point capillary apparatus. Specific optical rotations were measured in solution using sodium light at 589 nm where no absorption occurred for all compounds. Absorption spectra were recorded on a Cary-5000 spectrophotometer from Agilent Technologies. Photochromic reactions were induced *in situ* by a continuous irradiation Hg/Xe lamp (Hamamatsu, LC6- or LC8-Lightningcure, 200 W) equipped with narrow band interference filters of appropriate wavelengths: Semrock BP-370/36 for λ_{irr} = 370 nm, Semrock FF01-438/24-25 for λ_{irr} = 438 nm, Semrock FF01-485/20-25 for λ_{irr} = 485 nm. The irradiation power was measured using a photodiode from Ophir (PD300-UV) and corrected after a measurement with an additional Schott long pass filter (LP-545) to measure NIR contribution (P_{LP}) that is let through the Semrock filter (P_{Total}), considering a 90% transmittance: $P_{\lambda irr} = P_{Total} - (10/9 \times P_{LP})$. The photoconversion reaction was followed by a combination of ^{1}H NMR and UV-visible absorption spectra, realized by successive irradiations at 370 nm (438 or 485 nm). The *E*/*Z* ratios were determined by integration of the azobenzene proton signals of each isomer. A quartz cell of 10 mm path length has been used for solution measurement.

Isothermal titration calorimetry: LecA was expressed and purified as previously described. [39] All experiments were performed at 25 °C with an ITC200 isothermal titration calorimeter (Microcal-Malvern Panalytical, Grenoble, France). The lyophilized LecA protein was dissolved in a buffer

composed of 20 mM Tris·HCl (pH 7.5), 100 mM NaCl and 100 μM $CaCl_2$ with 5% or 10% DMSO final. All compounds were first dissolved in DMSO then in same buffer for a final concentration of 5% or 10% DMSO. The 200 μL sample cell containing LecA (concentrations ranging from 200 to 300 μM) was subjected to injections of ligand solution: 20 injections of 2 μL (2-3 mM, depending on the ligand) at intervals of 120s while stirring at 850 rpm. Control experiments were performed by repeating the same protocol, but injecting the ligand into buffer solution. The supplied software Origin 7 or MicroCal PEAQ-ITC was used to fit the experimental data to a theoretical titration curve allowing the determination of affinity (i.e., dissociation constant, K_d), binding enthalpy (ΔH), and stoichiometry (n). Values for free energy change (ΔG) and entropy contributions (TΔS) were derived from the equation $\Delta G = \Delta H - T\Delta S = - RT \ln K_d$ (with T = 298.15 K and R = 8.314 J $mol^{-1}K^{-1}$).

General procedure I for the *O*-alkylation with $BrCH_2CH_2NHBoc$: A solution of glycosyl azobenzene (1.0 equiv.) in anhydrous DMF (~3.5 mL per mmol) was added K_2CO_3 (2.0-4 equiv.) and $BocNHCH_2CH_2Br$ (1.5-4 equiv.), then stirred for overnight at 60°C. After the reaction was completed (TLC monitoring), the solvent was evaporated to dryness under reduced pressure. The residue was dissolved in EtOAc, neutralized with HCl (1 M), and extracted with EtOAc (3 times). The organic phase was washed with brine, dried over anhydrous Na_2SO_4, evaporated under reduced pressure in vacuo, and purified by CombiFlash Rf+ (CH_2Cl_2/MeOH = 15/1).

General procedure II for the Boc deprotection: To a solution of Boc-protected compound in anhydrous MeOH (~10 mL per mmol) was added dropwise AcCl (1.0-3.0 equiv.) at 0°C, slowly warmed to rt and stirred overnight. After the reaction was completed (TLC monitoring), the solvent was evaporated to dryness under reduced pressure. The residue was dissolved in MeOH, acetone was added, and a precipitate was obtained, which was washed with CH_2Cl_2 and n-pentane successively to give a pure compound.

General procedure III for the syhthesis of *S*-galactosyl azobenzenes: A round bottom flask was charged with Xantphos Pd-G_3 (5 mol %), acetylated β-thiogalactoside **13** [35] (1.1 equiv) and iodinated azobenzene (1 equiv). After Ar flushing, dry THF (0.25 M) was added and the mixture stirred for 5 min before NEt_3 (1.1 equiv.) was added. The reaction mixture was stirred at rt under Ar for 6-8 h, diluted with EtOAc, filtered over celite and washed with EtOAc. The collected organic layers were concentrated under reduced pressure, and purified by flash chromatography (cyclohexane/EtOAc = 7/3) to give thioglycoside.

General procedure IV for the Zemplén deacetylation: To a seal tube containing galactose derivatives in dry MeOH (0.15 M), NaOMe (30 mol %, 0.5 M sol. in MeOH) was added. The mixture was stirred at room temperature until total deprotection. The solution was neutralized using Amberlite IR-120 (H), filtered, concentrated and used without further purification to give the product in quantitative yield.

(***E*)-4-[4′-(2-tert-Butyloxycarbonylaminoethyloxy)-phenylazo)phenyl-β-D-galactopyranoside (*E*-8):** From **7** [26] (100 mg, 0.26 mmol) and $BocNHCH_2CH_2Br$ (87 mg, 0.39 mmol), K_2CO_3 (72 mg, 0.52 mmol) according to the General procedure I, compound **8** (123 mg, 91%) was isolated as a yellow solid. Rf = 0.5 (CH_2Cl_2/MeOH = 5/1), mp: 132°C, $[\alpha]_D^{23}$: -28.6 (*c* = 0.5, MeOH); ^{1}H NMR (400 MHz, CD_3OD): δ 7.85 (d, *J* = 9.2 Hz, 2H, H_{Ph}), 7.83 (d, *J* = 9.2 Hz, 2H, H_{Ph}), 7.23 (d, *J* = 9.2 Hz, 2H, H_{Ph}), 7.07 (d, *J* = 8.8 Hz, 2H, H_{Ph}), 4.97 (d, *J* = 8.0 Hz, 1H, H_1), 4.09 (t, *J* = 5.6 Hz, 2H, OCH_2), 3.92 (d, *J* = 3.2 Hz, 1H, H_4), 3.83 (dd, *J* = 10.0, 7.6 Hz, 1H, H_6), 3.81-3.71 (m, 3H, $H_{2,5,6'}$), 3.61 (dd, *J* = 9.6, 3.2 Hz, 1H, H_3), 3.46 (t, *J* = 6.0 Hz, 2H, NCH_2), 1.45 (s, 9H, $3\times CH_3$); ^{13}C NMR (100 MHz, CD_3OD): δ 162.6, 161.1, 149.3, 148.4 (Cq); 125.4, 125.1, 118.0, 115.9 (CH_{Ph}); 102.6 (C_1); 77.1 ($C_{2\text{ or }5}$); 74.8 (C_3); 72.2 ($C_{5\text{ or }2}$); 70.2 (C_4); 68.3 (OCH_2); 62.4 (C_6); 40.9 (NCH_2); 28.7 (CH_3). HRMS (ESI) *m/z*: Calcd for $C_{25}H_{34}N_3O_9$ $[M+H]^+$: 520.2290, Found 520.2281.

(*E*)-4-[4′-(2-Aminoethyloxy)-phenylazo)phenyl-β-D-galacto-pyranoside·HCl (*E*-1): From **8** (70 mg, 0.13 mmol) and AcCl (11 mg, 0.13 mmol) according to the General procedure II, compound **1** (34 mg, 58%) was isolated as a yellow solid. mp: 226°C, $[\alpha]_D^{23}$: -49.0 (*c* = 0.2, H_2O); ^{1}H NMR (400 MHz, CD_3OD): δ 7.90 (d, *J* = 7.2 Hz, 2H, H_{Ph}), 7.85 (d, *J* = 8.8 Hz, 2H, H_{Ph}), 7.24 (d, *J* = 9.2 Hz, 2H, H_{Ph}), 7.16 (d, *J* = 9.2 Hz, 2H, H_{Ph}), 4.98 (d, *J* = 7.6 Hz, 1H, H_1), 4.32 (t, *J* = 4.8 Hz, 2H, OCH_2), 3.92 (d, *J* = 3.2 Hz, 1H, H_4), 3.85 (dd, *J* = 9.6, 7.6 Hz, 1H, H_6), 3.81-3.74 (m, 3H, $H_{2,5,6}$), 3.61 (dd, *J* = 10.0, 3.6 Hz, 1H, H_3), 3.40 (t, *J* = 5.2 Hz, 2H, NCH_2); ^{13}C NMR (100 MHz, CD_3OD): δ 161.5, 161.3, 149.2, 148.9

(Cq); 125.5, 125.2, 118.0, 116.0 (CH_{Ph}); 102.6 (C_1); 77.1 ($C_{2\ or\ 5}$); 74.8 (C_3); 72.2 ($C_{5\ or\ 2}$); 70.2 (C_4); 65.6 (OCH_2); 62.4 (C_6); 40.3 (NCH_2); HRMS (ESI) *m/z*: Calcd for $C_{20}H_{26}N_3O_7$ $[M+H]^+$: 420.1765, Found 420.1763.

(*E*)-3-(3′-Hydroxy-phenylazo)phenyl-β-D-galactopyranoside (*E*-10): To a solution of D-galactose (500 mg, 2.77 mmol) in water (20 mL) was added 3,3'-dihydroxyazobenzene **9** [33] (1.78 g, 8.33 mmol, 3.0 equiv.) and Et_3N (10.4 mL, 74.79 mmol) at -10 °C. After stirring for 10 min, DMC (2.8 g, 16.60 mmol) was added and stirred for another 2 h. Et_3N (10.4 mL) was added again at -10°C and stirred for 10 min, then DMC (2.8 g) was added and stirred for 2 h. after repeating one again the addtition of Et_3N and DMC, and stirred for 2 h, the reaction was completed as monitored by TLC. Aqueous NH_4OH solution (3×10 mL) was added and co-evaporated to remove $Et_3HN^+Cl^-$ at 50 °C. The residue was further purified by CombiFlash Rf+ (eluted with EtOAc/MeOH = 15/1) to afford the compound **9** as an orange solid (416 mg, 40%), along with 1.42 g of recovered azobenzene **8** (80%). Rf = 0.43 (CH_2Cl_2/MeOH = 5/1), mp: 78°C, $[\alpha]_D^{23}$: -60.8 (*c* = 1.0, MeOH); ^{1}H NMR (400 MHz, CD_3OD): δ 7.64 (t, *J* = 2.4 Hz, 1H, H_{Ph}), 7.58 (dt, *J* = 8.4, 0.8 Hz, 1H, H_{Ph}), 7.46 (t, *J* = 8.0 Hz, 1H, H_{Ph}), 7.42 (dt, *J* = 8.0, 1.6 Hz, 1H, H_{Ph}), 7.35 (t, *J* = 7.6 Hz, 1H, H_{Ph}), 7.30 (t, *J* = 2.4 Hz, 1H, H_{Ph}), 7.26 (ddd, *J* = 8.0, 2.0, 0.4 Hz, 1H, H_{Ph}), 6.94 (ddd, *J* = 8.0, 2.4, 0.6 Hz, 1H, H_{Ph}), 4.97 (d, *J* = 7.6 Hz, 1H, H_1), 3.92 (d, *J* = 3.6 Hz, 1H, H_4), 3.85 (dd, *J* = 9.6, 8.0 Hz, 1H, H_6), 3.82-3.73 (m, 3H, $H_{2,5,6'}$), 3.61 (dd, *J* = 10.0, 3.6 Hz, 1H, H_3); ^{13}C NMR (100 MHz, CD_3OD): δ 159.9, 159.4, 155.1, 155.0 (Cq); 130.9, 120.6, 119.5, 118.9, 116.8, 110.8, 108.9 (CH_{Ph}); 103.0 (C_1); 77.0 ($C_{2\ or\ 5}$); 74.8 (C_3); 72.2 ($C_{2\ or\ 5}$); 70.2 (C_4); 62.4 (C_6); HRMS (ESI) *m/z*: Calcd for $C_{18}H_{21}N_2O_7$ $[M+H]^+$: 377.1343, Found 377.1341.

(*E*)-3-[3′-(2-tert-Butyloxycarbonylaminoethyloxy)-phenylazo)phenyl-β-D-galactopyranoside (*E*-11): From **10** (200 mg, 0.53 mmol) and $BocNHCH_2CH_2Br$ (475 mg, 2.12 mmol), K_2CO_3 (293 mg, 2.12 mmol) according to the General procedure I, compound **11** (220 mg, 80%) was isolated as an orange solid. Rf = 0.5 (CH_2Cl_2/MeOH = 5/1), mp: 90°C, $[\alpha]_D^{23}$: -29.0 (*c* = 0.5 , MeOH); ^{1}H NMR (400 MHz, CD_3OD): δ 7.66 (t, *J* = 2.4 Hz, 1H, H_{Ph}), 7.60 (ddd, *J* = 8.0, 1.6, 0.8 Hz, 1H, H_{Ph}), 7.53 (d, *J* = 8.4 Hz, 1H, H_{Ph}), 7.48-7.42 (m, 3H, H_{Ph}), 7.27 (ddd, *J* = 8.4, 2.4, 0.8 Hz, 1H, H_{Ph}), 7.10 (ddd, *J* = 8.0, 2.4, 0.8 Hz, 1H, H_{Ph}), 4.97 (d, *J* = 7.6 Hz, 1H, H_1), 4.09 (t, *J* = 5.2 Hz, 2H, OC*H*$_2$), 3.93 (d, *J* = 3.2 Hz, 1H, H_4), 3.88-3.70 (m, 4H, $H_{2,5,6,6'}$), 3.62 (dd, *J* = 9.6, 3.2 Hz, 1H, H_3), 3.47 (t, *J* = 5.2 Hz, 2H, NC*H*$_2$), 1.44 (s, 9H, 3×C*H*$_3$); ^{13}C NMR (100 MHz, CD_3OD): δ 160.9, 160.0, 158.5, 154.9 (Cq); 131.0, 130.9, 120.8, 119.1, 119.0, 118.2, 110.9, 107.8 (CH_{Ph}); 102.9 (C_1); 80.2 (Cq); 77.0 ($C_{2\ or\ 5}$); 74.7 (C_3); 72.2 ($C_{5\ or\ 2}$); 70.1 (C_4); 68.2 (OCH_2); 62.3 (C_6); 41.0 (NCH_2); 28.7 (CH_3); HRMS (ESI) *m/z*: Calcd for $C_{25}H_{34}N_3O_9$ $[M+H]^+$: 520.2290, Found 520.2286.

(*E*)-3-[3′-(2-Aminoethyloxy)-phenylazo)phenyl-β-D-galactopyranoside·HCl (*E*-2): From **11** (200 mg, 0.38 mmol) and AcCl (45 mg, 0.57 mmol) according to the General procedure II, compound **2** (80 mg, 46%) was isolated as a yellow solid, along with 93 mg of recovered compound **11** (47%). mp: 140°C, $[\alpha]_D^{23}$: -46.1 (*c* = 0.5, H_2O) ; ^{1}H NMR (400 MHz, CD_3OD): δ 7.67 (t, *J* = 1.6 Hz, 1H, H_{Ph}), 7.63-7.60 (m, 2H, H_{Ph}), 7.55-7.46 (m, 3H, H_{Ph}), 7.29 (ddd, *J* = 8.4, 2.4, 0.4 Hz, 1H, H_{Ph}), 7.20 (ddd, *J* = 8.4, 2.4, 0.6 Hz, 1H, H_{Ph}), 4.97 (d, *J* = 7.6 Hz, 1H, H_1), 4.33 (t, *J* = 4.8 Hz, 2H, OC*H*$_2$), 3.93 (d, *J* = 3.2 Hz, 1H, H_4), 3.87-3.73 (m, 4H, $H_{2,5,6,6'}$), 3.61 (dd, *J* = 9.6, 3.2 Hz, 1H, H_3), 3.41 (t, *J* = 5.2 Hz, 2H, NC*H*$_2$); ^{13}C NMR (100 MHz, CD_3OD): δ 160.2, 160.0, 155.1, 154.9 (Cq); 131.3, 131.0, 120.9, 119.2, 119.1, 119.0, 110.9, 107.8 (CH_{Ph}); 103.0 (C_1); 77.1 ($C_{2\ or\ 5}$); 74.8 (C_3); 72.3 ($C_{5\ or\ 2}$); 70.2 (C_4); 65.5 (OCH_2); 62.4 (C_6); 40.3 (NCH_2); HRMS (ESI) *m/z*: Calcd for $C_{20}H_{26}N_3O_7$ $[M+H]^+$: 420.1765, Found 420.1762.

(*E*)-4-(4′-Hydroxy-phenylazo)phenyl-2,3,4,6-tetra-*O*-acetyl-β-S-D-galactopyranoside (*E*-14): From Xantphos Pd-G_3 (22 mg, 0.023 mmol), **13** (186 mg, 0.51 mmol), azobenzene **12** [36,37] (150 mg, 0.46 mmol) and NEt_3 (71 µL, 0.51 mmol) in THF (2 mL) according to the General procedure III, compound **14** was obtained as a brown solid (234 mg, 90%). *Rf* = 0.5 (cyclohexane/EtOAc = 1/1), mp: 155.1°C; $[\alpha]_D^{22}$ = + 6.0 (*c* = 0.1, $CDCl_3$); ^{1}H NMR (300 MHz, $CDCl_3$): δ 7.85 (d, *J* = 8.7 Hz, 2H, H_{Ph}), 7.80 (d, *J* = 8.4 Hz, 2H, H_{Ph}), 7.62 (d, *J* = 8.5 Hz, 2H, H_{Ph}), 6.93 (d, *J* = 8.8 Hz, 2H, H_{Ph}), 5.44 (d, *J* = 3.3 Hz, 1H, H_4), 5.29 (t, *J* = 9.9 Hz, 1H, H_2), 5.09 (dd, *J* = 9.9, 3.3 Hz, 1H, H_3), 4.80 (d, *J* = 10.0 Hz, 1H, H_1), 4.18 (qd, *J* = 11.5, 6.7 Hz, 2H, $H_{6,6'}$), 3.99 (t, *J* = 6.4 Hz, 1H, H_5), 2.13 (s, 3H, C*H*$_3$), 2.11 (s, 3H, C*H*$_3$), 2.06 (s, 3H, C*H*$_3$), 1.98 (s, 3H, C*H*$_3$); ^{13}C NMR (75 MHz, $CDCl_3$): δ 170.7, 170.4, 170.3,

169.8, 159.1, 152.2, 147.1, 135.1 (Cq); 132.6, 125.3, 123.1, 116.0 (CH_{Ph}); 86.1 (C_1); 74.8 (C_5); 72.2 (C_3); 67.4 ($C_{2,4}$); 61.9 (C_6); 21.0, 20.8, 20.8, 20.7 (CH_3); HRMS (ESI) *m/z*: calcd for $C_{26}H_{28}N_2O_{10}S$ $[M+H]^+$ 561.1537, Found 561.1545.

(*E*)-4-(4′-Hydroxy-phenylazo)phenyl-β-S-D-galactopyranoside (*E*-15): From **14** (156 mg, 0.28 mmol) and MeONa (280 µL, 0.14 mmol) according to the General procedure IV, compound **15** was obtained as a brown solid (105 mg, >99%). *Rf* = 0.4 (CH_2Cl_2/MeOH = 8:2), mp: 215°C; $[\alpha]_D^{22}$ = -100.0 (*c* = 0.1, MeOH); ^{1}H NMR (300 MHz, CD_3OD): δ 7.91-7.77 (m, 4H, H_{Ph}), 7.76-7.66 (m, 2H, H_{Ph}), 7.02-6.91 (m, 2H, H_{Ph}), 4.77 (d, *J* = 9.7 Hz, 1H, H_1), 3.99 (dd, *J* = 3.3, 1.1 Hz, 1H, H_4), 3.92-3.64 (m, 4H, $H_{2,5,6,6'}$), 3.60 (dd, *J* = 9.1, 3.3 Hz, 1H, H_3); ^{13}C NMR (75 MHz, CD_3OD): δ 162.2, 152.6, 147.5, 139.3 (Cq); 131.6, 125.9, 123.7, 116.8 (CH_{Ph}); 89.5 (C_1); 80.7 (C_5); 76.4 (C_3); 71.0 (C_2); 70.5 (C_5); 62.7 (C_6); HRMS (ESI) *m/z*: calcd for $C_{18}H_{20}N_2O_6S$ $[M+H]^+$ 393.1115, Found 393.1117.

(*E*)-4-[4′-(2-tert-Butyloxycarbonylaminoethyloxy)-phenylazo)phenyl-β-S-D-galactopyranoside (*E*-16): From **15** (79 mg, 0.20 mmol) and $BocNHCH_2CH_2Br$ (212 mg, 0.50 mmol), K_2CO_3 (56 mg, 0.4 mmol) according to the General procedure I, compound **16** (95 mg, 88%) was isolated as a yellow solid. Rf = 0.3 (CH_2Cl_2/MeOH = 10/1), mp: 159°C, $[\alpha]_D^{23}$: -65.6 (*c* = 0.5, MeOH); ^{1}H NMR (400 MHz, CD_3OD): δ 7.88 (d, *J* = 8.8 Hz, 2H, H_{Ph}), 7.80 (d, *J* = 8.4 Hz, 2H, H_{Ph}), 7.66 (d, *J* = 8.4 Hz, 2H, H_{Ph}), 7.08 (d, *J* = 9.2 Hz, 2H, H_{Ph}), 4.73 (d, *J* = 9.6 Hz, 1H, H_1), 4.10 (t, *J* = 5.6 Hz, 2H, OC*H*$_2$), 3.94 (d, *J* = 3.2 Hz, 1H, H_4), 3.79 (dd, *J* = 11.2, 6.8 Hz, 1H, H_6), 3.72 (dd, *J* = 11.2, 5.2 Hz, 1H, $H_{6'}$), 3.71-3.68 (m, 1H, H_5), 3.66 (d, *J* = 9.2 Hz, 1H, H_2), 3.57 (dd, *J* = 9.2, 3.6 Hz, 1H, H_3), 3.46 (t, *J* = 5.6 Hz, 2H, NC*H*$_2$), 1.44 (s, 9H, 3×C*H*$_3$); ^{13}C NMR (100 MHz, CD_3OD): δ 162.9, 158.5, 152.5, 148.3, 140.0 (Cq); 131.3, 125.7, 123.9, 115.9 (CH_{Ph}); 89.4 (C_1); 80.8 ($C_{2\text{ or }5}$); 80.3 (Cq); 76.3 (C_3); 70.9 ($C_{5\text{ or }2}$); 70.5 (C_4); 68.3 (OCH_2); 62.7 (C_6); 40.9 (NCH_2); 28.7 (CH_3); HRMS (ESI) *m/z*: Calcd for $C_{25}H_{34}N_3O_8S$ $[M+H]^+$: 536.2061, Found 536.2057.

(*E*)-4-[4′-(2-Aminoethyloxy)-phenylazo)phenyl-β-S-D-galactopyranoside·HCl (*E*-3): From **16** (45 mg, 0.08 mmol) and AcCl (20 mg, 0.25 mmol) according to the General procedure II, compound **3** (35 mg, 90%) was isolated as a yellow solid. Mp: 224°C, $[\alpha]_D^{23}$: -91.0 (*c* = 0.1, H_2O); ^{1}H NMR (400 MHz, CD_3OD): δ 7.92 (d, *J* = 8.4 Hz, 2H, H_{Ph}), 7.81 (d, *J* = 8.4 Hz, 2H, H_{Ph}), 7.67 (d, *J* = 8.4 Hz, 2H, H_{Ph}), 7.17 (d, *J* = 9.2 Hz, 2H, H_{Ph}), 4.74 (d, *J* = 9.6 Hz, 1H, H_1), 4.33 (t, *J* = 4.8 Hz, 2H, OC*H*$_2$), 3.93 (d, *J* = 2.8 Hz, 1H, H_4), 3.80 (dd, *J* = 11.6, 6.8 Hz, 1H, H_6), 3.73 (dd, *J* =11.6, 5.2 Hz, 1H, $H_{6'}$), 3.70-3.64 (m, 2H, $H_{2,5}$), 3.54 (dd, *J* = 9.2, 3.2 Hz, 1H, H_3), 3.42 (t, *J* = 4.8 Hz, 2H, NC*H*$_2$); ^{13}C NMR (100 MHz, CD_3OD): δ 161.9, 152.4, 148.8, 140.3 (Cq); 131.2, 125.7, 124.0, 116.1 (CH_{Ph}); 89.3 (C_1); 80.8 ($C_{2\text{ or }5}$); 76.3 (C_3); 70.9 ($C_{5\text{ or }2}$); 70.5 (C_4); 65.6 (OCH_2); 62.7 (C_6); 40.3 (NCH_2); HRMS (ESI) *m/z*: Calcd for $C_{20}H_{26}N_3O_6S$ $[M+H]^+$: 436.1537, Found 436.1535.

(*E*)-3-(4′-Hydroxy-phenylazo)phenyl-2,3,4,6-tetra-*O*-acetyl-β-S-D-galactopyranoside (*E*-18): From Xantphos Pd-G_3 (19 mg, 0.02 mmol), **13** (161 mg, 0.44 mmol), azobenzene **17** [36,37] (130 mg, 0.4 mmol) and NEt_3 (65 µL, 0.44 mmol) in THF (1.65 mL) according to the General procedure III, compound **18** was obtained as an orange solid (219 mg, 98%). *Rf* = 0.5 (cyclohexane/EtOAc = 1:1), mp 170°C; $[\alpha]_D^{22}$ = -33.0 (*c* = 0.1, $CDCl_3$); ^{1}H NMR (300 MHz, $CDCl_3$): δ 8.03 (t, *J* = 1.9 Hz, 1H, H_{Ph}), 7.93-7.82 (m, 2H, H_{Ph}), 7.82-7.77 (m, 1H, H_{Ph}), 7.55 (dt, *J* = 7.8, 1.5 Hz, 1H, H_{Ph}), 7.44 (t, *J* = 7.8 Hz, 1H, H_{Ph}), 6.99-6.85 (m, 2H, H_{Ph}), 5.44 (dd, *J* = 3.4, 1.1 Hz, 1H, H_4), 5.30 (t, *J* = 9.9 Hz, 1H, H_2), 5.09 (dd, *J* = 9.9, 3.3 Hz, 1H, H_3), 4.82 (d, *J* = 9.9 Hz, 1H, H_1), 4.21-4.11 (m, 2H, $H_{6,6'}$), 3.99 (ddd, *J* = 7.0, 5.8, 1.1 Hz, 1H, H_5), 2.11 (s, 3H, CH_3), 2.09 (s, 3H, CH_3), 1.99 (s, 3H, CH_3), 2.00(s, 3H, CH_3); ^{13}C NMR (75 MHz, $CDCl_3$): δ 170.4, 170.5, 170.3, 169.7, 159.0, 153.2, 147.1, 133.9, 133.8, 129.6, 125.9 (Cq); 125.3, 122.7, 116.0 (CH_{Ph}); 86.5 (C_1); 74.7 (C_5); 72.2 (C_3); 67.5 ($C_{2,4}$); 61.9 (C_6);, 21.0, 20.8, 20.7 (CH_3); HRMS (ESI) *m/z* calcd for $C_{26}H_{28}N_2O_{10}S$ $[M+H]^+$ 561.1537, found 561.1544.

(*E*)-3-(4′-Hydroxy-phenylazo)phenyl-β-S-D-galactopyranoside (*E*-19): From **18** (218 mg, 0.39 mmol) and MeONa (390 µL, 0.19 mmol) according to the General procedure IV, compound **19** was obtained as a red solid (150 mg, >99%). *Rf* = 0.3 (CH_2Cl_2/MeOH = 8:2); mp: 187.5°C; $[\alpha]_D^{22}$ = -22.0 (*c* = 0.05, MeOH); ^{1}H NMR (300 MHz, CD_3OD): δ 8.09-8.03 (m, 1H, H_{Ph}), 7.90-7.82 (m, 2H, H_{Ph}), 7.77-7.71 (m, 1H, H_{Ph}), 7.69-7.63 (m, 1H, H_{Ph}), 7.48 (t, *J* = 7.9 Hz, 1H, H_{Ph}), 7.00-6.90 (m, 2H, H_{Ph}), 4.72 (d, *J* = 9.6 Hz, 1H, H_1), 3.97 (dd, *J* = 3.3, 1.0 Hz, 1H, H_4), 3.89-3.62 (m, 4H, $H_{2,5,6,6'}$), 3.57 (dd, *J* = 9.2, 3.3 Hz, 1H, H_3); ^{13}C NMR (75 MHz, CD_3OD): δ 147.5, 137. 5, 133.5, 130.4 (Cq); 126.1, 124.9, 122.6,

116.8 (CH_{Ph}); 90.0 (C_1); 80.6 (C_5); 76.4 (C_3); 71.0 (C_2); 70.4 (C_4); 62.6 (C_6); HRMS (ESI) *m/z*: calcd for $C_{18}H_{20}N_2O_6S$ $[M+H]^+$ 393.1115, Found 393.1189.

(*E*)-3-[4′-(2-tert-Butyloxycarbonylaminoethyloxy)-phenylazo)phenyl-β-S-D-galactopyranoside (*E*-20): From **19** (150 mg, 0.38 mmol) and $BocNHCH_2CH_2Br$ (213 mg, 0.95 mmol), K_2CO_3 (157 mg, 1.14 mmol) according to the General procedure I, compound **20** (101 mg, 50%) was isolated as an orange solid. Rf = 0.28 (CH_2Cl_2/MeOH = 10/1), mp: 114°C, $[\alpha]_D^{23}$: -36.1 (*c* = 0.5, MeOH); ^{1}H NMR (400 MHz, CD_3OD): δ 8.05 (t, *J* = 2.0 Hz, 1H, H_{Ph}), 7.91 (d, *J* = 9.2 Hz, 2H, H_{Ph}), 7.74 (ddd, *J* = 7.6, 1.6, 0.4 Hz, 1H, H_{Ph}), 7.65 (dt, *J* = 8.0, 0.8 Hz, 1H, H_{Ph}), 7.46 (t, *J* = 8.0 Hz, 1H, H_{Ph}), 7.09 (d, *J* = 8.4 Hz, 2H, H_{Ph}), 4.69 (d, *J* = 9.6 Hz, 1H, H_1), 4.11 (t, *J* = 5.2 Hz, 2H, OCH_2), 3.92 (d, *J* = 2.8 Hz, 1H, H_4), 3.80 (dd, *J* = 11.6, 7.2 Hz, 1H, H_6), 3.73 (dd, *J* = 11.6, 5.2 Hz, 1H, $H_{6'}$), 3.68-3.61 (m, 2H, $H_{2,5}$), 3.52 (dd, *J* = 8.8, 3.2 Hz, 1H, H_3), 3.47 (t, *J* = 5.6 Hz, 2H, NCH_2), 1.45 (s, 9H, 3×CH_3); ^{13}C NMR (100 MHz, CD_3OD): δ 163.1, 158.5, 154.2, 148.2, 137.6 (Cq); 133.5, 130.5, 125.9, 124.8, 122.7, 115.9 (CH_{Ph}); 90.0 (C_1); 80.6 (C_5); 80.3 (Cq); 76.3 (C_3); 71.0 (C_2); 70.4 (C_4); 68.3 (OCH_2); 62.5 (C_6); 40.9 (NCH_2); 28.7 (CH_3); HRMS (ESI) *m/z*: Calcd for $C_{25}H_{34}N_3O_8S$ $[M+H]^+$: 536.2061, Found 536.2055.

(*E*)-3-[4′-(2-Aminoethyloxy)-phenylazo)phenyl-β-S-D-galactopyranoside·HCl (*E*-4): From **20** (47 mg, 0.087 mmol) and AcCl (20 mg, 0.26 mmol) according to the General procedure II, compound **1** (35 mg, 85%) was isolated as an orange solid. mp: 208°C, $[\alpha]_D^{23}$: -17.9 (*c* = 0.2, H_2O); ^{1}H NMR (400 MHz, CD_3OD): δ 8.06 (t, *J* = 1.6 Hz, 1H, H_{Ph}), 7.96 (d, *J* = 8.8 Hz, 2H, H_{Ph}), 7.75 (dt, *J* = 8.4, 1.2 Hz, 1H, H_{Ph}), 7.67 (dt, *J* = 7.6, 1.6 Hz, 1H, H_{Ph}), 7.47 (t, *J* = 8.4 Hz, 1H, H_{Ph}), 7.18 (d, *J* = 8.8 Hz, 2H, H_{Ph}), 4.69 (d, *J* = 10.0 Hz, 1H, H_1), 4.33 (t, *J* = 5.2 Hz, 2H, OCH_2), 3.92 (d, *J* = 3.2 Hz, 1H, H_4), 3.80 (dd, *J* = 11.6, 7.2 Hz, 1H, H_6), 3.73 (dd, *J* = 11.6, 5.2 Hz, 1H, $H_{6'}$), 3.68-3.61 (m, 2H, $H_{2,5}$), 3.52 (dd, *J* = 9.2, 3.2 Hz, 1H, H_3), 3.42 (t, *J* = 5.2 Hz, 2H, NCH_2); ^{13}C NMR (100 MHz, CD_3OD): δ 162.1, 154.2, 148.7, 137.7 (Cq); 133.7, 130.6, 125.9, 124.8, 122.8, 116.1 (CH_{Ph}); 89.9 (C_1); 80.6 (C_5); 76.3 (C_3); 71.0 (C_2); 70.4 (C_4); 65.6 (OCH_2); 62.6 (C_6); 40.2 (NCH_2); HRMS (ESI) *m/z*: Calcd for $C_{20}H_{26}N_3O_6S$ $[M+H]^+$: 436.1537, Found 436.1537.

(*E*)-2-(4′-Hydroxy-phenylazo)phenyl-2,3,4,6-tetra-*O*-acetyl-β-S-D-galactopyranoside (*E*-22): From Xantphos Pd-G_3 (24.5 mg, 0.0255 mmol), **13** (204 mg, 0.56 mmol), azobenzene **21** [36,37] (165 mg, 0.51 mmol) and NEt_3 (65 µL, 0.44 mmol) in THF (2.1 mL) according to the General procedure III, compound **22** was obtained as an orange solid (167 mg, 54%). *Rf* = 0.5 (cyclohexane/EtOAc = 1:1), mp: 165.6°C; $[\alpha]_D^{22}$ = - 42.0 (*c* = 0.1, $CDCl_3$); ^{1}H NMR (300 MHz, $CDCl_3$): δ 7.92-7.84 (m, 2H, H_{Ph}), 7.71-7.60 (m, 2H, H_{Ph}), 7.37-7.32 (m, 2H, H_{Ph}), 7.00-6.90 (m, 2H, H_{Ph}), 5.47 (dd, *J* = 3.4, 1.1Hz, 1H, H_4), 5.40 (t, *J* = 10.0Hz, 1H, H_2), 5.10 (dd, *J* = 9.9, 3.4 Hz, 1H, H_3), 4.99 (d, *J* = 10.1Hz, 1H, H_1), 4.18-4.10 (m, 2H, $H_{6,6'}$), 4.00 (ddd, *J* = 7.1, 5.9, 1.1 Hz, 1H, H_5), 2.17 (s, 3H, CH_3), 2.03 (s, 3H, CH_3), 1.99 (s, 3H, CH_3), 1.97 (s, 3H, CH_3); ^{13}C NMR (75 MHz, $CDCl_3$): δ 170.6, 170.5, 170.3, 169.8, 159.4, 150.9, 147.2, 130.6, 130.4, 127.8, 125.6, 117.6, 116.1(CH_{Ph}); 85.3 (C_1); 74.7 (C_5); 72.3 (C_3); 67.6 (C_2);, 67.5 (C_4); 61.9 (C_6); 21.2, 20.9, 20.8, 20.7 (CH_3); HRMS (ESI) *m/z*: calcd for $C_{26}H_{28}N_2O_{10}S$ $[M+H]^+$ 561.1537, Found 561.1543.

(*E*)-2-(4′-Hydroxy-phenylazo)phenyl-β-S-D-galactopyranoside (*E*-23): From **22** (156 mg, 0.28 mmol) and MeONa (280 µL, 0.14 mmol) according to the General procedure IV, compound **23** was obtained as a brown solid (105 mg, >99%). *Rf* = 0.2 (CH_2Cl_2/MeOH = 4/1); mp: 175.3°C; $[\alpha]_D^{22}$ = +43.0 (*c* = 0.1, MeOH); ^{1}H NMR (300 MHz, CD_3OD): δ 7.95-7.90 (m, 2H, H_{Ph}), 7.81 (dd, *J* = 8.0, 1.3 Hz, 1H, H_{Ph}), 7.66 (dd, *J* = 8.0, 1.5 Hz, 1H, H_{Ph}), 7.48-7.40 (m, 1H, H_{Ph}), 7.37-7.27 (m, 1H, H_{Ph}), 7.04-6.93 (m, 2H, H_{Ph}), 4.92 (d, *J* = 9.7 Hz, 1H, H_1), 4.04 (dd, *J* = 3.3 Hz, 1H, H_4), 3.91-3.73 (m, 4H, $H_{2,5,6,6'}$), 3.66 (dd, *J* = 9.1, 3.3 Hz, 1H, H_3); ^{13}C NMR (75 MHz, CD_3OD): δ 177.8, 138.1, 131.8, 129.8, 127.1, 126.4, 117.4, 116.8 (CH_{Ph}); 87.5 (C_1); 80.5 (C_5); 76.4 (C_3); 71.1 (C_2); 70.6 (C_4); 62.7 (C_6); HRMS (ESI) *m/z*: calcd for $C_{18}H_{20}N_2O_6S$ $[M+Na]^+$ 415.0934, Found 415.0941.

(*E*)-2-[4′-(2-*Tert*-butyloxycarbonylaminoethyloxy)-phenylazo)phenyl-β-S-D-galactopyranoside (*E*-24): From **23** (30 mg, 0.076 mmol) and $BocNHCH_2CH_2Br$ (26 mg, 0.12 mmol), K_2CO_3 (21 mg, 0.15 mmol) according to the General procedure I, compound **24** (35 mg, 88%) was isolated as an orange solid after purification by CombiFlash Rf+ (CH_2Cl_2/MeOH = 20/1). Rf = 0.3 (CH_2Cl_2/MeOH = 10/1), mp: 124°C, $[\alpha]_D^{23}$: +95.4 (*c* = 0.1, MeOH); ^{1}H NMR (400 MHz, CD_3OD): δ 7.91 (d, *J* = 8.8 Hz, 2H, H_{Ph}), 7.74 (d, *J* = 6.8 Hz, 1H, H_{Ph}), 7.61 (dd, *J* = 8.0, 1.6 Hz, 1H, H_{Ph}), 7.39 (td, *J* = 7.6, 2.0 Hz, 1H, H_{Ph}),

7.24 (td, J = 8.0, 0.8 Hz, 1H, H_{Ph}), 7.08 (d, J = 8.8 Hz, 2H, H_{Ph}), 4.86 (d, J = 9.6 Hz, 1H, H_1), 4.10 (t, J = 5.6 Hz, 2H, OCH_2), 3.94 (d, J = 3.2 Hz, 1H, H_4), 3.80-3.68 (m, 4H, $H_{2,5,6,6'}$), 3.57 (dd, J = 9.2, 3.6 Hz, 1H, H_3), 3.46 (t, J = 5.6 Hz, 2H, NCH_2), 1.44 (s, 9H, 3×CH_3); ^{13}C NMR (100 MHz, CD_3OD): δ 163.1, 158.5, 150.7, 148.6, 139.0 (Cq); 132.2, 129.4, 126.9, 126.4, 117.3, 115.9 (CH_{Ph}); 87.3 (C_1); 80.7 (C_5); 80.3 (Cq); 76.4 (C_3); 71.1 (C_2); 70.5 (C_4); 68.3 (OCH_2); 62.7 (C_6); 40.9 (NCH_2); 28.7 (CH_3); HRMS (ESI) *m/z*: Calcd for $C_{25}H_{34}N_3O_8S$ $[M+H]^+$: 536.2061, Found 536.2057.

(*E*)-2-[4′-(2-Aminoethyloxy)-phenylazo)phenyl-β-S-D-galactopyranoside·HCl (*E*-5): From **24** (55 mg, 0.10 mmol) and AcCl (24 mg, 0.30 mmol) according to the General procedure II, compound **5** (36 mg, 77%) was isolated as a green solid. mp: 204°C, $[\alpha]_D^{23}$: +14.3 (c = 0.3, H_2O); ^{1}H NMR (400 MHz, CD_3OD): δ 7.96 (d, J = 8.8 Hz, 2H, H_{Ph}), 7.76 (dd, J = 8.4, 1.2 Hz, 1H, H_{Ph}), 7.63 (dd, J = 7.6, 1.2 Hz, 1H, H_{Ph}), 7.42 (td, J = 7.6, 1.6 Hz, 1H, H_{Ph}), 7.26 (td, J = 8.0, 1.2 Hz, 1H, H_{Ph}), 7.17 (d, J = 9.2 Hz, 2H, H_{Ph}), 4.89-4.88 (m, 1H, H_1), 4.34 (t, J = 4.8 Hz, 2H, OCH_2), 3.96 (d, J = 3.2 Hz, 1H, H_4), 3.81-3.71 (m, 4H, $H_{2,5,6,6'}$), 3.58 (dd, J = 9.2, 3.2 Hz, 1H, H_3), 3.42 (t, J = 4.8 Hz, 2H, NCH_2); ^{13}C NMR (100 MHz, CD_3OD): δ 162.1, 150.6, 149.1, 139.2 (Cq); 132.4, 129.4, 126.9, 126.2, 117.3, 116.1 (CH_{Ph}); 87.2 (C_1); 80.7 (C_5); 76.4 (C_3); 71.1 (C_2); 70.5 (C_4); 65.7 (OCH_2); 62.7 (C_6); 40.2 (NCH_2); HRMS (ESI) *m/z*: Calcd for $C_{20}H_{26}N_3O_6S$ $[M+H]^+$: 436.1537, Found 436.1535.

Acknowledgements

Y. Fan gratefully acknowledges China Scholarship Council (CSC) for a doctoral scholarship. The authors thank the Centre National de la Recherche Scientifique (CNRS) for support of this research and MRES for a doctoral fellowships to A. El Rhaz. The authors would like to thank also Cyril Colas from the "Fédération de Recherche" ICOA/CBM (FR2708)" for HRMS analysis.

Supporting Information

Absorption spectra, determination of the molar absorption coefficients, copy of ^{1}H NMR spectra of photoisomerization, half-life time measurements, corrected concentration for ITC measurement, copy of ^{1}H and ^{13}C NMR spectra of all new compounds (PDF).

References

1. Cassini A.; Högberg L. D.; Plachouras D.; Quattrocchi A.; Hoxha A.; Skov Simonsen G.; Colomb-Cotinat M.; Kretzschmar M. E.; Devleesschauwer B.; Cecchini M.; Ait Ouakrim D.; Cravo Oliveira T.; Struelens M. J.; Suetens C.; Monnet D. L.; Burden of AMR Collaborative Group. *Lancet Infect. Dis.* **2019**, *19*, 56-66. doi: org/10.1016/S1473-3099(18)30605-4.
2. Pelegrin A. C.; Palmieri M.; Mirande C.; Oliver A.; Moons P.; Goossens H.; van Belkum A. *FEMS Microbiology Rev*. **2021**, *45*, 1-20. doi: org/10.1093/femsre/fuab026
3. Tacconelli E.; Carrara E.; Savoldi, A.; Harbarth, S.; Mendelson, M.; Monnet, D. L.; Pulcini, C.; Kahlmeter, G.; Kluytmans, J.; Carmeli, Y.; Ouellette, M.; Outterson, K.; Patel, J.; Cavaleri, M.; Cox, E. M.; Houchens, C. R.; Grayson, M. L.; Hansen, P.; Singh, N.; Theuretzbacher, U.; Magrini, N.; WHO Pathogens Priority List Working Group. *Lancet Infect. Dis.* **2018**, *18*, 318-327. doi: org/10.1016/S1473-3099(17)30753-3
4. Chemani, C.; Imberty, A.; De Bentzmann, S.; Pierre, M.; Wimmerová, M.; Guery, B. P.; Faure, K. *Infect Immun.* **2009**, *77*, 2065-2075. doi: org/10.1128/IAI.01204-08
5. Wojtczak, K.; Byrne, J. P. *ChemMedChem* **2022**, *17*, e202200081. doi: org/10.1002/cmdc.202200081

6. Zahorska, E.; Rosato, F.; Stober, K.; Kuhaudomlarp, S.; Meiers, J.; Hauck, D.; Reith, D.; Gillon, E.; Rox, K.; Imberty, A.; Römer, W.; Titz, A. *Angew. Chem. Int. Ed.* **2023**, *62*, e202215535. doi: org/10.1002/anie.202215535
7. Siebs, E.; Shanina, E.; Kuhaudomlarp, S.; Da Silva Figueiredo Celestino Gomes, P.; Fortin, C.; Seeberger, P. H.; Rognan, D.; Rademacher, C.; Imberty, A.; Titz, A. *ChemBioChem* **2022**, *23*, e202100563. doi: org/10.1002/cbic.202100563
8. Mała, P.; Siebs, E.; Meiers, J.; Rox, K.; Varrot, A.; Imberty, A.; Titz, A. *J. Med. Chem.* **2022**, *65*, 14180-14200. doi: org/10.1021/acs.jmedchem.2c01373
9. Behren, S.; Westerlind, U. *Eur. J. Org. Chem.* **2023**, *26*, e202200795. doi: org/10.1002/ejoc.202200795
10. Leusmann, S.; Ménová, P.; Shanin, E.; Titz, A.; Rademacher, C. *Chem. Soc. Rev.* **2023**, *52*, 3663-3740. doi: org/10.1039/D2CS00954D
11. Lerch, M. M.; Hansen, M. J.; van Dam, G. M.; Szymanski, W.; Feringa, B. L. *Angew. Chem. Int. Ed.* **2016**, *55*, 10978-10999. doi: org/10.1002/anie.201601931
12. Yu, Z.; Hecht, S. *Chem. Commun.* **2016**, *52*, 6639-6653. doi: org/10.1039/C6CC01423B
13. Velema, W. A.; Szymanski, W.; Feringa, B. L. *J. Am. Chem. Soc.* **2014**, *136*, 2178-2191. doi: org/10.1021/ja413063e
14. Broichhagen, J.; Frank, J. A.; Trauner, D. *Acc. Chem. Res.* **2015**, *48*, 1947-1960. doi: org/10.1021/acs.accounts.5b00129
15. Hüll, K.; Morstein, J.; Trauner, D. *Chem. Rev.* **2018**, *118*, 10710-10747. doi: org/10.1021/acs.chemrev.8b00037
16. Fuchter, M. J. *J. Med. Chem.* **2020**, *63*, 11436-11447. doi: org/10.1021/acs.jmedchem.0c00629
17. Weber, T.; Chandrasekaran, V.; Stamer, I.; Thygesen, M. B.; Terfort, A.; Lindhorst, T. K. *Angew. Chem. Int. Ed.* **2014**, *53*, 14583-14586. doi.org/10.1002/anie.201409808
18. Chandrasekaran, V.; Jacob, H.; Petersen, F.; Kathirvel, K.; Tuczek, F.; Lindhorst, T. K. *Chem. Eur. J.* **2014**, *20*, 8744-8752. doi: org/10.1002/chem.201402075
19. Möckl, L.; Müller, A.; C. Bräuchle C.; Lindhorst, T. K. *Chem. Commun*. **2016**, *52*, 1254-1257. DOI: 10.1039/c5cc08884d
20. Despras, G.; Möckl, L.; Heitmann, A.; Stamer, I.; Bräuchle, C.; Lindhorst, T. K. *ChemBioChem* **2019**, *20*, 2373-2382. doi: org/10.1002/cbic.201900269
21. Ponader, D.; Igde, S.; Wehle, M.; Märker, K.; Santer, M.; Bléger, D.; Hartmann, L. *Beilstein J. Org. Chem.* **2014**, *10*, 1603-1612. doi:10.3762/bjoc.10.166
22. Hu, Y.; Beshr, G.; Garvey, C. J.; Tabor, R. F.; Titz, A.; Wilkinson, B. L. *Colloids and Surf. B: Biointerfaces* **2017**, *159*, 605-612. doi: org/10.1016/j.colsurfb.2017.08.016
23. Osswald, U.; Boneberg, J.; Wittmann, V. *Chem. Eur. J.* **2022**, *28*, e202200267. doi: org/10.1002/chem.202200267
24. Lin, C.; Maisonneuve, S.; Métivier, R.; Xie, J. *Chem. Eur. J.* **2017**, *23*, 14996-15001. doi: org/10.1002/chem.201703461
25. Lin, C.; Jiao, J.; Maisonneuve, S.; Mallétroit, J.; Xie, J. *Chem. Commun.* **2020**, *56*, 3261-3264. doi: org/10.1039/C9CC09853D
26. Wang, Z.; Maisonneuve, S.; Xie, J. *J. Org. Chem.* **2022**, *87*, 16165-16174. doi: org/10.1021/acs.joc.2c01511
27. Jiao, J.; Maisonneuve, S.; Xie, J. *J. Org. Chem.* **2022**, *87*, 8534-8543. doi: org/10.1021/acs.joc.2c00652
28. Bruneau, A.; Gillon, E.; Furiga, A.; Brachet, E.; Alami, M.; Roques, C.; Varrot, A.; Imberty, A.; Messaoudi, S. *Eur. J. Med. Chem.* **2023**, *247*, 115025. doi: org/10.1016/j.ejmech.2022.115025

29. Gajdos, L.; Blakeley, M. P.; Haertlein, M.; Forsyth, V. T.; Devos, J. M.; Imberty, A. *Nature Commun.* **2022**, *13*, 194. doi: org/10.1038/s41467-021-27871-8
30. Cioci, G.; Mitchell, E. P.; Gautier, C.; Wimmerová, M.; Sudakevitz, D.; Pérez, S.; Gilboa-Garber, N.; Imberty, A. *FEBS Lett.* **2003**, *555*, 297-301. doi: org/10.1016/S0014-5793(03)01249-3
31. Kadam, R. U.; Garg, D.; Schwartz, J.; Visini, R.; Sattler, M.; Stocker, A.; Darbre, T.; Reymond, J.-L. *ACS Chem. Biol.* **2013**, *8*, 1925-1930. doi: org/10.1021/cb400303w
32. Sommer, R.; Wagner, S.; Rox, K.; Varrot, A.; Hauck, D.; Wamhoff, E.-C.; Schreiber, J.; Ryckmans, T.; Brunner, T.; Rademacher, C.; Hartmann, R. W.; Brönstrup, M.; Imberty, A.; Titz, A. *J. Am. Chem. Soc.* **2018**, *140*, 2537-2545. doi: org/10.1021/jacs.7b11133
33. Rodrigue, J.; Ganne, G.; Blanchard, B.; Saucier, C.; Giguère, D.; Shiao, T. C.; Varrot, A.; Imberty, A.; Roy, R. *Org. Biomol. Chem.* **2013**, *11*, 6906-6918. doi: org/10.1039/c3ob41422a
34. Gund, S. H.; Shelkar, R. S.; Nagarkar, J. M. *RSC Adv.* **2014**, *4*, 42947-42951. doi: org/10.1039/C4RA06027J
35. Bruneau, A.; Roche, M.; Hamze, A.; Brion, J.; Alami, M.; Messaoudi, S. *Chem. Eur. J.* **2015**, *21*, 8375-8379. doi: org/10.1002/chem.201501050
36. Schultzke, S.; Walther, M.; Staubitz, A. *Molecules* **2021**, *26*, 3916. doi: org/10.3390/molecules26133916
37. Ngaini, Z.; Hissam, M. A.; Mortadza, N. A.; Abd Halim, A. N.; Daud, A. I. *Nat. Prod. Res.* **2023**, 1486310 (1-11). doi: org/10.1080/14786419.2023.2262713
38. Dam, T. K.; Brewer, C. F. *Chem. Rev.* **2002**, *102*, 387-430. doi: org/10.1021/cr000401x
39. Kuhaudomlarp, S.; Gillon, E.; Varrot, A.; Imberty, A. Methods Mol. Biol. **2020**, *2132*, 257-266. doi: org/10.1007/978-1-0716-0430-4_25